The Prime Focus Imaging Spectrograph for the Southern African Large Telescope: Operational Modes

Henry A. Kobulnicky[a], Kenneth H. Nordsieck[a], Eric B. Burgh[a],
Michael P. Smith[a], Jeffrey W. Percival[a] , Ted B. Williams[b], and Darragh O'Donoghue[c]
[a]University of Wisconsin, Madison, [b]Rutgers University, [c]South African Astrophysical Observatory

ABSTRACT

The Prime Focus Imaging Spectrograph (PFIS) will be the workhorse first-generation spectrograph on the Southern African Large Telescope (SALT). Scheduled for commissioning in late 2004, PFIS is a versatile high-throughput imaging spectrograph with a complement of 5 volume-phase holographic gratings for spectroscopic programs from 3200 Å to 9000 Å at resolutions of R=1500 to R=10000. A magazine of 6 longslits and 30 custom laser-milled slitmasks enables single- or multi-object spectroscopy over an 8 arc minute diameter field. With the gratings stowed, a dual-etalon Fabry-Perot subsystem enables imaging spectroscopy at R=500, R=3000, and R=12,500. The polarization subsystem, consisting of a polarizing beam-splitter used in conjunction with half- and quarter-wave plates, allows linear or circular polarimetric measurements in ANY of the spectroscopic modes. Three mosaiced rapid-readout frame-transfer CCDs provide the capability for time-resolved sampling at rates in excess of 10 Hz. Combinations of these subsystems permit novel observing modes for specialized scientific programs. Examples include high time-resolution multi-object spectral polarimetry of accreting compact objects, and Fabry-Perot polarimetry or imaging spectral polarimetry of nebulae and stellar clusters. The demands of queue-scheduled observing on a fixed-altitude telescope require that the instrument be capable of rapid reconfiguration between modes.

Keywords: Astronomical spectrographs, optical design, near-ultraviolet spectroscopy, volume phase holographic gratings, Fabry-Perot interferometry, spectropolarimetry

1. INSTRUMENT OVERVIEW

The Prime Focus Imaging Spectrograph (PFIS) will be the workhorse first-generation, all-purpose spectrograph on the Southern African Large Telescope (SALT). The optical design of PFIS is described elsewhere in this volume[1].
The nominal field of view is 8'. The plate scale at the focal plane is 224 microns/arcsec.

PFIS is designed as a facility-class, general-purpose spectrograph with many capabilities including medium-band imaging, Fabry-Perot narrow-band imaging, longslit grating spectroscopy and multi-slit grating spectroscopy. Linear and circular polarimetry may be performed in any of the imaging or spectroscopic modes at the expense of halving the field of view. Furthermore, the frame-transfer CCDs[2] enable rapid readouts or charge shuffling so that very high time- resolutions in excess of 0.1 s are possible at the cost of restricted areal coverage. These diverse capabilities, combined with the excellent short-wavelength throughput, enable specialized observational programs such as time-resolved spectropolarimetric studies of energetic phenomena like close binaries, active galactic nuclei, and gamma ray bursts. This report provides an overview of the operational capabilities of PFIS and some anticipated science drivers.

The observational modes are most easily described in terms of the four major instrument subsystems: 1) the focal plane slits and masks, 2) the dispersive elements, consisting of either the complement of volume-phase holographic gratings or Fabry-Perot Etalon, 3) Polarization optics consisting of a ½ wave plate, a ¼ wave plate, and a polarizing beamsplitter , and 4) the array of 3 charge-transfer CCDs. Permutations of these mechanisms combine to give PFIS the versatility to address a broad range of astrophysical research programs. Table 1 summarizes the observational modes permitted by combinations of these four subsystems.

[a]*chip@astro.wisc.edu, khn@sal.wisc.edu, ebb@sal.wisc.edu, smith@sal.wisc.edu, jwp@sal.wisc.edu, Space Astronomy Laboratory, University of Wisconsin, Madison, 53706 [b]Department of Physics & Astronomy, Rutgers, Piscataway, NJ 08855, [c]dod@saao.ac.za, South African Astrophysical Observatory Observatory 7935, South Africa

Table 1: PFIS Operational Modes

	Imaging				Grating Spectroscopy			
CCD Readout Mode	Observing Mode	Focal Plane Unit	Field	Waveplate	Observing Mode	Focal Plane Unit	Field	Waveplate
Normal Readout (<0.25 Hz)	Filter Imaging	none	8’	N	Longslit Spectroscopy	slits 1-6	8’	N
	Fabry-Perot Imaging	none	8’	N	Multi-slit Spectroscopy	mask	8’	N
	Imaging Polarimetry	Mask 2	4’	Y	Longslit Spectropolarimetry	slit 7	4’	Y
	Fabry-Perot Polarimetry	Mask 2	4’	Y	Multi-slit Spectropolarimetry	mask	4’	Y
Frame Transfer (fast; ~1 Hz)	Fast Filter Imaging	Mask 1	4’	N	Fast longslit Spectroscopy	slit 8	4’	N
	Fast Fabry-Perot Imaging	Mask 1	4’	N	Fast multi-slit Spectroscopy	mask	4’	N
	Fast Imaging Polarimetry	-	-	-	Fast Longslit Polarimetry	-	-	-
	Fast Fabry-Perot Polarimetry	-	-	-	Fast Longslit Spectropolarimetry	-	-	-
Charge Shuffle (very fast; up to 20 Hz)	V. Fast Filter Imaging	mask	”	N	V. Fast Longslit Spectroscopy	slits 1-8	”	N
	V. Fast Fabry-Perot Imaging	mask	”	N	V. Fast Multi-slit Spectroscopy	mask	”	N
	V. Fast Imaging Polarimetry	mask	”	Y	V. Fast Longslit Spectropolar.	slit 7	”	Y
	V. Fast Fabry-Perot Polarimetry	mask	”	Y	V. Fast Multi-slit Spectropolar.	mask	”	Y

Forbidden Modes

2. PFIS SUBSYSTEMS

2.1 Focal Plane Unit

The first PFIS subsystem in the light path is the focal plane. A jukebox adjacent to the focal plane stores up to 30 longslits and custom-designed masks. Insertion time is targeted to be <30 seconds. The choice of focal plane slit or mask depends on the science goals and operational mode desired. There are three options for the focal plane configuration.

i. Open - Direct imaging (and possibly objective prism work) are likely to be the only modes where there is no element in the focal plane. By implication, the camera is unarticulated. Acquisition and peak-up operations are performed by direct imaging or by the guide probes located on the perimeter of the PFIS focal plane aperture.

ii. Longslit - Most spectroscopic programs will use a single 8’ longslit in the focal plane. The longslits will be made of a reflective metal and tilted at an angle of 12 degrees to allow a slit-viewing device to image the focal plane. The reflective area of the slit will be approximately 2’ in the dispersion direction by the length of the slit in the cross-dispersion direction. Table 2 lists nine standard longslit plates which will always be available in the focal plane magazine. Slits 1-6 are 7.5’ in length and span a variety of widths to accommodate the full range of seeing expected. These will be used for standard longslit grating spectroscopy. Slit Plate #7 covers the central 4’ of the focal plane and is used for spectropolarimetry. It will be constructed with shims to allow a variety of slit widths. Slit #8 is 12” (128 pixels) long, covering the upper half of the FOV and is imaged onto the upper half of the CCD detector. This permits one half of the detector to be used as a storage buffer in frame-transfer mode during high time-resolution observations. This slit is used for high-speed spectroscopy and spectropolarimetry where only a small portion of the chip needs to be used. Slit plate #9 has a short 6” slit with a coronographic center for spectroscopy and spectropolarimetry in coronographic modes.

Table 2: Complement of Standard Longslits

Reflective Slit Plate #	Length	Width (“)
1	7.5’	0.45”
2	7.5’	0.6”
3	7.5’	0.9”
4	7.5’	1.1”
5	7.5’	1.3”
6	7.5’	3.0”
7	Central 4’	1.1” adjustable for spectral polarimetry
8	4’ above CTB	1.1” adjustable for high speed spectroscopy
9	4’’	1.1” w/ coronographic center

The mean site seeing informs the distribution of longslit widths. A variety of slits should be available to cover the range of atmospheric seeing conditions expected at the site. For the SALT telescope, the median seeing is 0.9” at zenith. Seeing varies approximately as FWHM $\propto \sec(z)^{0.6}$. For SALT, where the zenith distance is always 37±6 degrees, the factor by which seeing is degraded from zenith seeing is 1.14±0.05. Furthermore, imperfections in the telescope optical system (primary mirror plus spherical aberration corrector, SAC) deliver a finite-sized image, assumed here to be characterized by a Gaussian PSF with FWHM=0.6”. The focal plane image size is the zenith image size convolved with the effects of atmosphere at 37 degree zenith distance and the telescope optics. Figure 1 shows the fraction of energy from a point source which is transmitted by a focal plane slit for three different slit widths as a function of image FWHM.

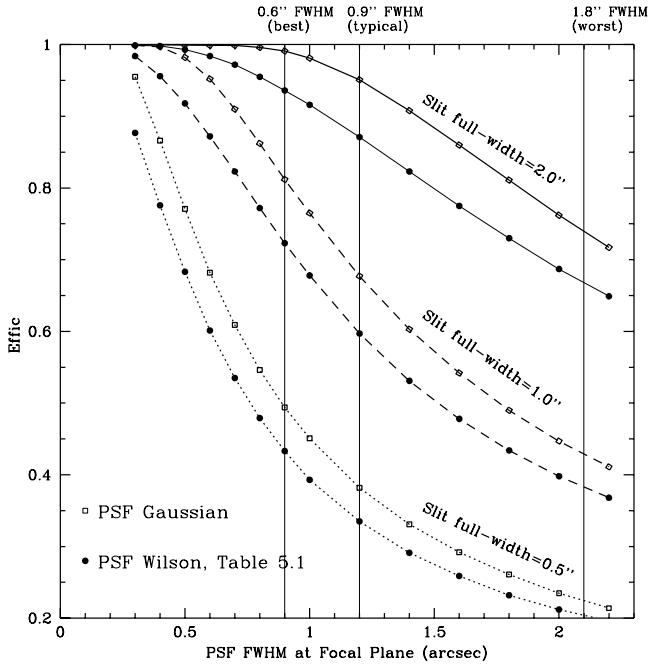

Figure 1. This Figure illustrates the fraction of energy from a point source which is transmitted by a focal plane slit for three different slit widths as a function of image FWHM. The solid line shows the enslitted energy fraction for a slit diameter of 2.0”. Open squares represent the case of a Gaussian PSF while filled circles represent the more realistic (i.e., long exposure) case when the PSF is given by the theoretical atmospheric profile.[3] The dashed line illustrates the comparison between the enslitted energy fraction for the two profiles for a slit width of 1.0”. The dotted line illustrates the case of a slit width of 0.5”. Thin vertical lines indicate the seeing at zenith for the best (0.6”), median (0.9”) and worst 10% (1.8”) conditions at the SALT site in Southerland, South Africa.

iii. Slitmask – Many science programs use custom laser-cut slitmasks to perform multi-object spectroscopy or multi-object spectropolarimetry. The masks will be milled with a micromachining laser mill and placed in a slitmask magazine designed

to hold 30 masks. Mask insertion time will be < 30 s. User-designed slitmasks will be cut and stored on-site and labeled with a bar-code to identify the mask and mask holder (frame) to be used with each mask. The focal plane plate scale of 224 microns/arcsec dictates that typical science slits (1.0 arcsec) will be very small (224 microns) and must be cut to extremely tight tolerances (few microns rms edge roughness). The slitmask manufacturing unit will be similar to the laser cutting systems adopted for the Gemini GMOS spectrograph[4]. Several standard masks will be available, including one which masks the upper and low quarter FOV for imaging polarimetry, and one which masks the lower half of the CCD for high time-resolution work. All high time-resolution imaging or Fabry-Perot modes require the use of a carbon-fiber mask in the focal plane to block the lower half of the field so that half of the CCD can be used as a storage buffer for frame-transfer operation (Mask 1). Imaging polarimetry and Fabry-Perot polarimetry require a mask to restrict the field of view to the central 4' (Mask 2).

Table 3: Standard Focal Plane Masks

Mask #	Configuration	Use
1	Masks lower 4' x 8'	High time-resolution imaging
2	Masks upper and lower 2' x 8' (central 4'x8' visible)	Imaging and Fabry-Perot polarimetry
3	1" pinholes spaced by 30" in cross-dispersion	Calibration
4+	Custom-cut science masks	Multi-slit spectroscopy

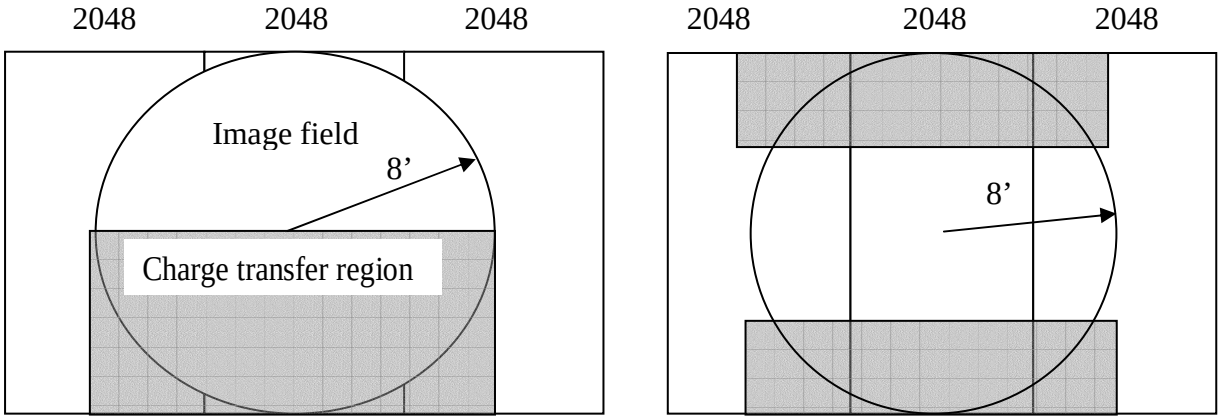

Figure 2. (*Left*) Schematic of the PFIS 8' field of view superimposed on the detector comprised of three 2048x4096 CCDs. Shaded area shows how the standard Slitmask #1 covers half the field when CCDs are used in frame transfer (fast readout) mode. (*Right*) Schematic of standard Slitmask #2 for use with all polarimetric modes. Only the central 4' of the 8' field is useable in polarimetric modes because the polarizing beamsplitter is used to image orthogonal polarizations onto the detector simultaneously**.**

2.2 Dispersive Elements

i. Imaging mode - No dispersive element is in the beam. This implies that the camera is in the unarticulated position. A special mode of spectropolarimetric imaging also uses this position, taking advantage of the lateral chromatic aberration in the camera to perform low-resolution spectropolarimetric imaging.

ii. Fabry-Perot Imaging - The etalon is the beam and the camera is at the unarticulated position. Estimated time for insertion of the etalons using a pneumatic piston is 30 s. Fabry-Perot imaging and Fabry-Perot polarimetry are modes that use this configuration. PFIS will have two F-P resolutions initially, a low-resolution (R=500-1000) tunable filter and a high-resolution (R=12000) mode. Low-resolution mode will use a single etalon with an interference filter to select the desired interference order. The high-resolution mode will use two etalon in series with the low-resolution etalon serving as the blocking filter to select the order for the high-resolution etalon. A third, medium-resolution etalon is planned as an upgrade path. Two of the three etalons will be installed in PFIS at any given time. The spectral range of the etalons will be 4300 Å to 8600 Å. Approximately 30 interference filters (R=50) will be required to isolate the FP orders over the entire spectral range. A subset of 15 of these will be installed in the filter magazine at any given time.

iii. Grating Spectroscopy - The majority of spectroscopic modes employ one of 6 gratings as the dispersive element. Longslit spectroscopy, multi-object spectroscopy, and spectropolarimetry are performed after selecting a grating from a magazine containing five volume-phase holographic (VPH) gratings and one conventional surface relief grating. Inserting time is designed to be <30 s. The grating complement is selected to cover the wavelength range of PFIS (3200 Å – 9000 Å) at a range of spectral resolutions from R=1000 to R=7000. Gratings have rule densities of 350 lines/mm, 780 l/mm, 1400 l/mm, 1800 l/mm, 2400 l/mm, and 3150 l/mm.

Figure 3 shows a contour plot of the efficiency of each grating as a function of wavelength and spectral resolution. Spectral resolutions are computed assuming a uniformly-filled slit with width 0.9". For pointlike sources, spectral resolutions will vary depending on both the slit width and the atmospheric seeing conditions. Smaller slits produce superior spectral resolutions, but at the cost of lower throughput. Figure 4 shows the tradeoff between slit width and spectral resolution for a variety of seeing conditions and slit widths. Two cases of good (0.7") and poor (1.2") seeing are depicted. Slit widths of 0.3", 0.5", 0.7", 1.0", 1.5", 2.0", and 2.5" are simulated. The four panels show the 780 l/mm, 1400 l/mm, 1800 l/mm and 2400 l/mm gratings at a representative wavelength where the efficiency is high.

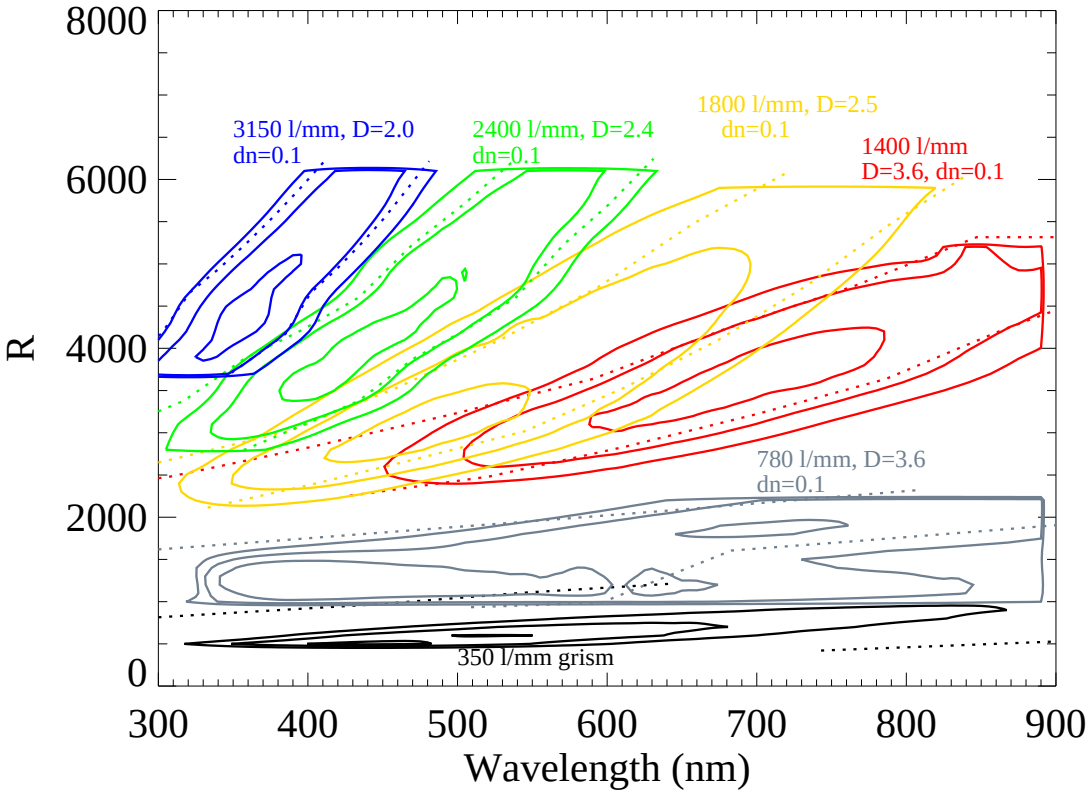

Figure 3. Contours of grating efficiency versus wavelength and spectral resolution for the complement of 6 PFIS gratings. Contours designate efficiencies of 90%, 70%, and 50%. Dotted lines show the approximate simultaneous wavelength coverage for single grating setting. "D" designates the thickness of each grating in microns and "dn" designates the modulation in the index of refraction of the VPH gratings. Resolutions assume a uniformly filled slit having a width of 0.9".

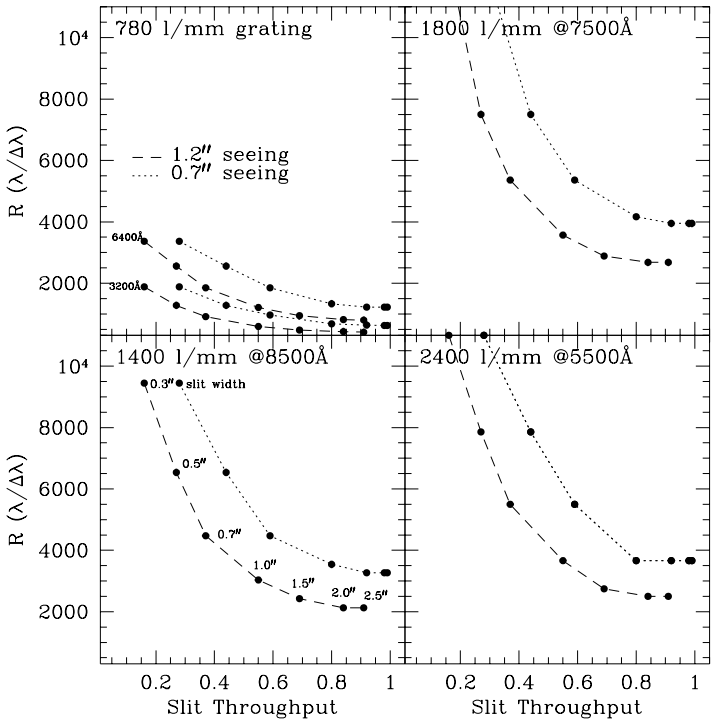

Figure 4. Tradeoff between spectral resolution and slit throughput for a point-like source as seen through the atmosphere and SALT telescope under excellent (0.7" at zenith) and poor (1.2" at zenith) seeing. Each panel shows a different PFIS VPH grating at the nominal wavelength of operation. Points in each graph denote slit widths of 0.3", 0.5", 0.7", 1.0", 1.5", 2.0", and 2.5".

2.3 Polarization Optics

The PFIS collimator includes a quarter-wave plate and a half-wave plate which may be inserted into the beam separately, for linear and circular polarization measurements, respectively. A polarizing beam splitter in the camera completes the polarimetric optics. The waveplates may also be used in series for "all-Stokes" polarimetric measurements. In "linear" Polarimetric mode, the half-wave plate steps through 8 position angles separated by 22.5 degrees in order to perform a complete linear polarization measurement. For circular polarization, two positions of the quarter-wave plate, in conjunction with 8 positions of the half-wave plate are required to complete a measurement. The waveplates may be used in conjunction with the Fabry-Perot etalon or the gratings and focal plane slits to perform spectropolarimetry. Polarimetric optics for PFIS are described in more detail elsewhere in this volume.[5]

2.4 CCD Subsystem

The detector is comprised of three mosaiced Marconi Applied Technologies 44-82 CCDs with 2048x4096 pixels and 15 micron pixels. Figure 2 shows a depiction of the 8' field of view projected onto the CCDs. The gap between CCDs is 15 pixels (225 microns). At the detector, the plate scale is 117 microns/arcsec so that, in most common applications, the detector will be binned 2x2 and still provide critical sampling of the point spread function. The detector will operate in 3 readout modes depending on the time sampling required.

i. Normal readout - The entire mini-mosaic, using 2x2 binning, can be read out in 3.6 s with $5e^-$/pix readout noise using 2 amplifiers per chip. A reduced readout noise of 3 e^-/pix can be achieved for lower readout rates, resulting in a read time of 11 s. Most science operation will occur in this "normal" readout mode.

ii. High Time-Resolution (fast readout) – The detectors may be operated in a "frame-transfer" mode whereby half of the detector is used as a storage buffer for the other half of the chip. The contents of the upper half of the chip can be transferred to the lower half of the chip in only 0.205 s. A second exposure may begin while the lower half of the chip is read out at the normal rate. In this mode, it is possible to obtain a continuous sequence of images with 1.8 s time resolution, but with the spatial field of view reduced to 4'.

iii. Charge Shuffle (very fast) – Charge shuffling in may be used in conjunction with telescope nods in order to perform high-quality sky subtraction for slit spectroscopy or off-band subtraction for Fabry-Perot imaging. In this mode, the charge is shuffled between pixel rows in an arbitrary fashion either during or between exposures. Alternatively, the chip may be windowed into arbitrary rectangular regions and read out at the maximum rate to achieve time resolutions as high as 0.1 s. Small groups of adjacent rows in the cross dispersion direction may be defined and used in conjunction with a longslit or slit mask to perform very high time-resolution spectroscopy. For example, an object may be placed just above the charge transfer boundary on the CCDs and all but 32 rows (when on-chip prebinning of 2x2 is used) of the detector are masked by a custom focal plane mask. The 32 rows are clocked continuously along the CCD columns toward the amplifiers at a limiting rate which is set by the readout time of 0.07 s (roughly 0.0017 s/row). In this manner, imaging or spectroscopy of single objects may be performed with time resolutions of 0.07 s. Images are smeared along the columns over time intervals of 0.0032 s, the time required to transfer 32 rows across the charge transfer boundary. Figure 5 illustrates schematically how this very fast readout mode would occur. Table 3 summarizes the readout times for a range of image heights using the frame transfer operations. Finally, charge shuffling may also be used to perform drift scan imaging by clocking the charge in the pixels at a sidereal rate.

Table 3. PFIS readout times as a function of image height.

Image Height (arcmin)	Image Height (pixels)	Transfer Time (s)	Store Transfer Time (s)	Readout Time (s)
4.0	2048	0.102	0.102	1.595
2.0	1024	0.051	0.051	0.797
0.5	256	0.013	0.013	0.199
0.125	64	0.003	0.003	0.050

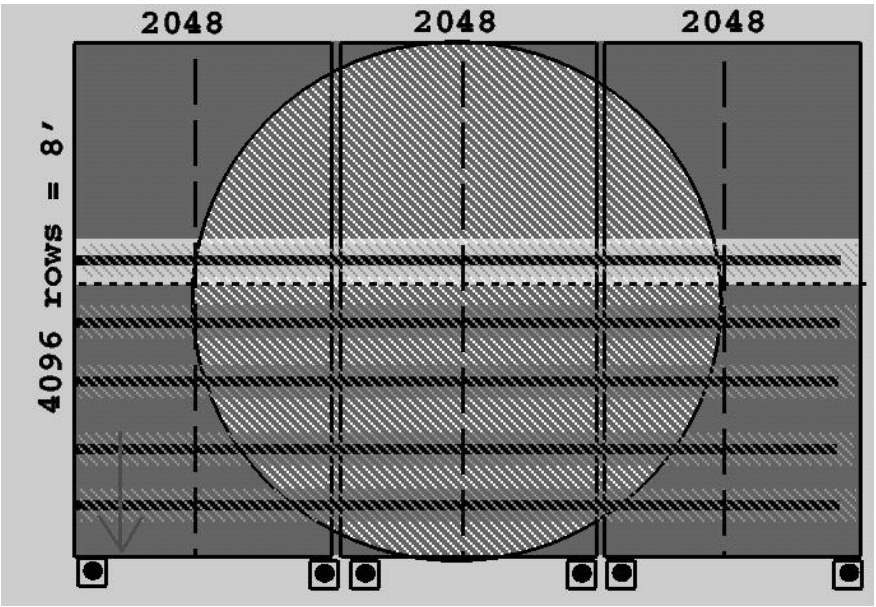

Figure 5. Schematic of very high speed spectroscopic operations using charge shuffling. An object is placed just above the charge transfer boundary (horizontal dotted line) which bisects each CCD. All but 64 rows of the CCD are masked with a custom mask. A spectrum is transferred below the charge transfer boundary every 0.05 s and then the CCD is read out at the maximum rate as a series of spectra are recorded. Time resolutions of 0.07 s are possible.

3. EXAMPLES OF SCIENCE CASES AND OPERATIONAL CONFIGURATIONS

Figure 6 shows the annulus of visibility for SALT as a function of declination and hour angle. Some common astronomical targets are labeled. Note that the Magellanic Clouds have visibility periods exceeding three hours, making them prime observational targets.

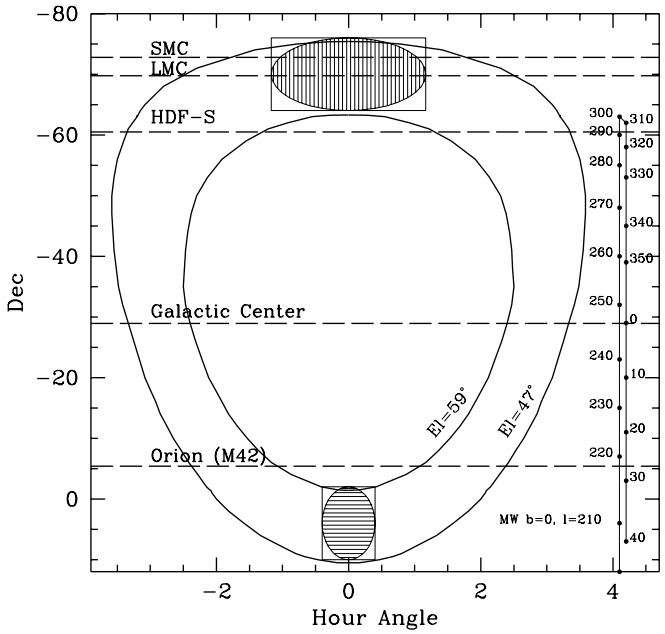

Figure 6. Annulus of total visibility for SALT as a function of declination and hour angle. Shaded ellipsoids mark the region of instantaneous visibility (6 degrees). The track at right indicates the relation between Galactic longitude and declination. It shows that much of the first quadrant and all of the fourth quadrant of the Galaxy is visible to SALT/PFIS.

3.1 Multi-Object Spectroscopy

Science Uses: Multi-object surveys in fields up to 8' diameter. Redshift surveys. Stellar Galactic and Magellanic Cloud surveys.

Target acquisition & guiding: By direct image with PFIS, then multi-stage peak-up process similar to other multi-object spectrographs. No focal plane viewing system is available when using multi-slit masks. Guiding uses offset guide probes located on the perimeter of the focal plane which view an annular region outside the 8' PFIS field.

Operational Sequence:

Afternoon

Flatfields with continuum lamp for calibration and location of alignment star boxes on slitmask. Moving baffle at pupil of spherical aberration corrector mimics pupil illumination during actual track.

Evening

1 Slew telescope and tracker to desired field (120 s)
2 Image of science field with SALTICAM or direct image with PFIS (10 s)
3 Insert slitmask (30 s)
4 Direct image with PFIS to verify field and mask alignment (10 s)
5 Fine-tune pointing and begin guiding with guide probes (20 s)
6 Insert and rotate grating to desired angle and articulate camera (30 s)
7 Start science exposures
8 Optional calibration lamp exposures using fiber-fed focal plane unit

Data rate: 6154 spectral pixels by 4096 spatial pixels in as little as 3.6 s

Limitations: Wavelength coverage on the detector varies with position of object in the field in the dispersion direction (as with all multi-object spectrographs using focal plane masks. Furthermore, the blaze of VPH gratings varies with angle of incidence. This means that the efficiency of the grating also varies with field position in the dispersion direction. Figure 7 illustrates this blaze shift for the case of the 780 l/mm grating and a 2' field angle.

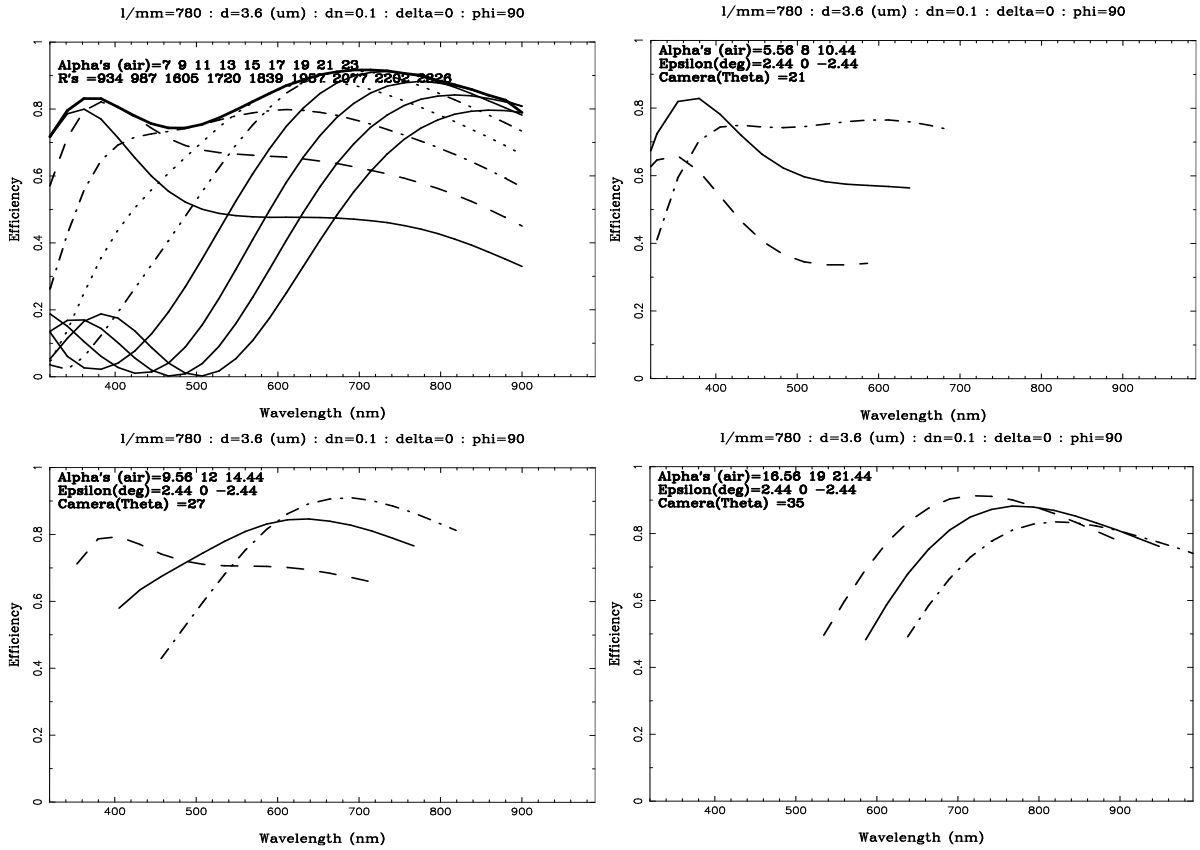

Figure 7. (upper left) Efficiency of the 780 l/mm VPH grating at 8 grating angles. Heavy line denotes the superblaze. Three additional panels show the simultaneous wavelength coverage and efficiency for an on-axis source (solid line) and two sources with cross dispersion field angles of 2' (dashed lines). Each panel illustrates a different grating angle corresponding to a different central wavelength.

3.2 High Time-resolution Circular Spectropolarimetry

Science Uses: Time-resolved single-object slit spectroscopy and spectropolarimetry of accreting objects, cataclysmic variables, active galactic nuclei, stellar flares, supernovae, gamma-ray bursts.

Target acquisition & guiding: By SALTICAM functioning as an acquisition camera viewing the reflective longslit plate.

Operational Sequence:

Afternoon

Flatfields with continuum lamp for calibration and location of alignment star boxes on slitmask. Moving baffle at pupil of spherical aberration corrector mimics pupil illumination during actual track.

Evening

1 Slew telescope and tracker to desired field (120 s)
2 Insert and rotate grating to desired angle and articulate camera (30 s)
3 Insert waveplates (20 s)
4 Insert longslit plate #8 (or #7) (30 s)
5 Visually select target & place it on slit while viewing slit with SALTICAM (10 s)
6 Fine-tune pointing and begin guiding with guide probes or directly on slit with SALTICAM (20 s)
7 Start science exposures
8 For x=1 to 8 positions of the ½ wave plate

a. Set ½ wave plate to position x
b. For y=1 to 2 positions of the ¼ wave plate
    i. Set ¼ waveplate to position y
    ii. Expose
    iii. Shuffle charge down by 32 rows
c. Readout bottom 32 rows near amplifier

9 Optional calibration lamp exposures using fiber-fed focal plane unit

Data rate: 6154 spectral pixels by 32 spatial pixels in as little as 0.07 s
Limitations: Multi-object capability is precluded in very high speed spectropolarimetric mode.

4. SENSITIVITY AND CALIBRATION ISSUES

PFIS is designed for extremely high throughput, especially shortward of 4000 Å, a region of the spectrum seldom exploited by today's large telescopes and spectrographs. Figure 8 shows the efficiency for components of the SALT and PFIS system. Peak efficiencies exceed 20% from 4000 Å to 8000 Å.

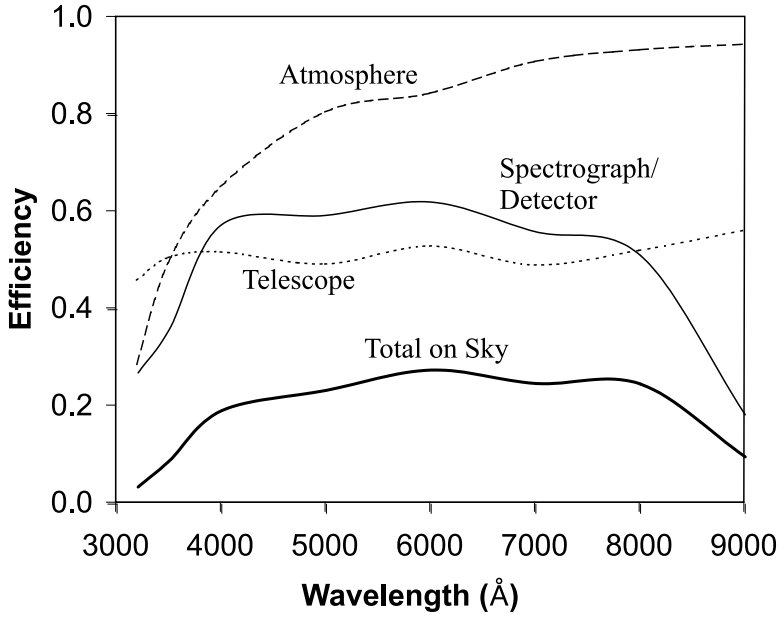

Figure 8. Total on-sky efficiency for PFIS on the SALT telescope as a function of wavelength. Due to the all-refractive optics and efficient VPH grating will allow PFIS to achieve superior sensitivity compared to existing 10 m class telescopes and spectrographs, especially shortward of 3500 Å.

Calibration, especially flat fielding, will be challenging due to the varying pupil illumination as an astronomical source tracks across the spherical primary. Flat fielding will be achieved using flats from an illuminated screen in the pupil of the spherical aberration corrector (SAC) in conjunction with a moving baffle in the SAC. Design studies have shown that a moving baffle at this location can mimic the effects of varying pupil illumination. The baffle will move at several times the sidereal rate so that flat fields can be rapidly acquired during the afternoon, either before or after a night's science observations.

Wavelength calibrations will be enabled by a fiber fed focal plane unit with a diffuser to uniformly illuminate the focal plane. The observatory will supply a collection of arc lamps for wavelength calibration fed by fiber optic from a room below the telescope structure.

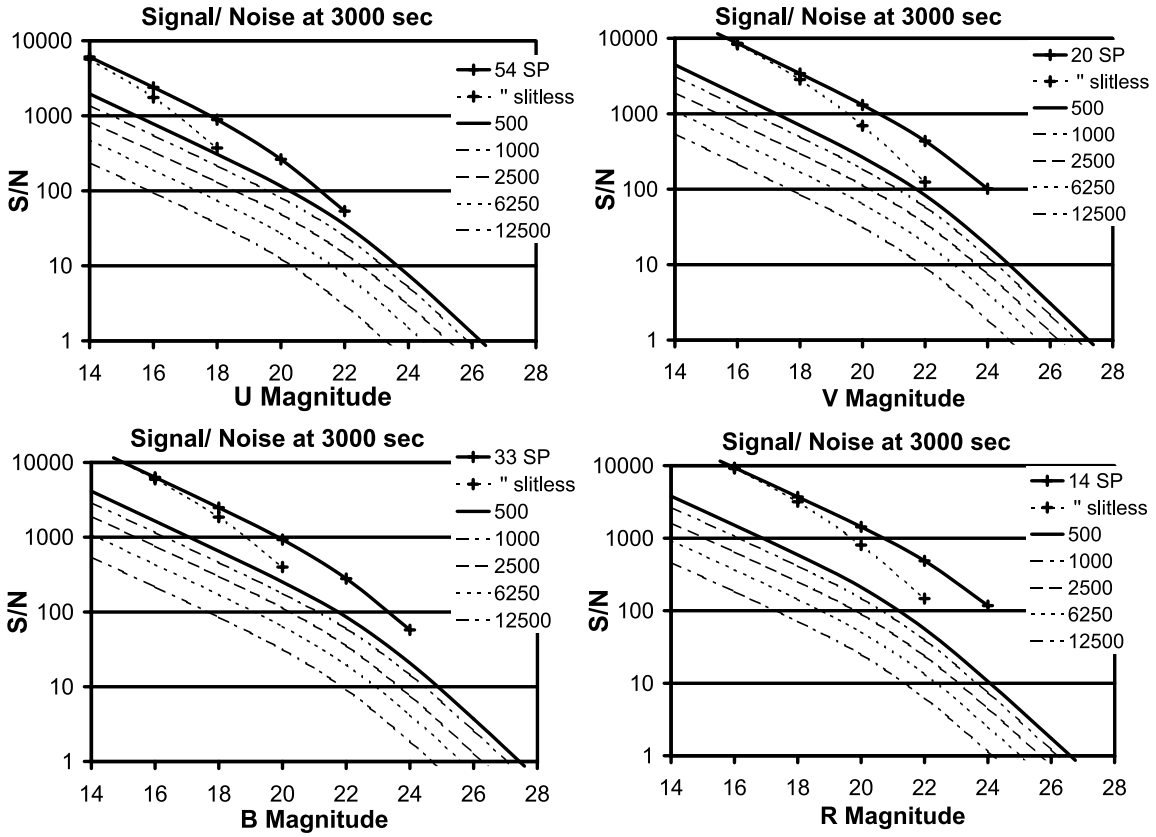

Figure 9. Signal-to-noise for PFIS+SALT as a function of continuum magnitude for a stellar source at spectral resolutions up to R=12500. A single exposure of 3000 s is assumed.

REFERENCES

1. Eric B. Burgh, Kenneth H. Nordsieck, Henry A. Kobulnicky, Ted B. Williams, Darragh O'Donoghue, Michael P. Smith, and Jeffry W. Percival, ``The Prime Focus Imaging Spectrograph for the Southern Afrtican Large Telescope: Optical Design,'' in *Instrument Design and Performance for Optical/Infreared Ground-Based Telescopes*, Proc. SPIE, vol 4841-164
2. Darragh O'Donoghue, D.B. Carter, G.P. Evans, W.P. Koorts, J.O'Conner, F. Osman, and S. can der Merwe, ``SALTICAM: $0.5 M acquisition camera: every big telescope should have one,'' in *Instrument Design and Performance for Optical/Infrared Ground-Based Telescopes*, Proc. SPIE, vol 4841, paper 52, 2002
3. R.N. Wilson, in *Reflecting Telescope Optics II*, 2002, New York-Springer-Verlag, p. 390
4. Kei Szeto, James R Stillburn, Tim Bond, Scott Roberts, Jerry Sebesta, and Leslie K. Saddlemyer, "Fabrication of Narrow Slit Masks for the Gemini Multi-Object Spectrograph, in *Optical Telescopes of Today and Tomorrow*, 1997, SPIE, 2871, p 1264
5. Kenneth H. Nordsieck, Kurt P. Jaehnig, Eric B. Burgh, Henry A. Kobulnicky, Jeffrey W. Percival, and Michael P. Smith, ``Instrumentation for high-resolution spectropolarimetry in the visible and far-ultraviolet'', in *Instrument Design and Performance for Optical/Infrared Ground-Based Telescopes*, Proc. SPIE, vol 4843- 24